AD-A153 630 FATIGUE BEHAVIOR OF HY-130 STEEL WELDMENTS CONTAINING FABRICATION DISCONTINUITIES(U) NAVAL RESEARCH LAB WASHINGTON DC S J GILL ET AL. 18 APR 85 NRL-MR-5520 1/1

UNCLASSIFIED F/G 20/11 NL

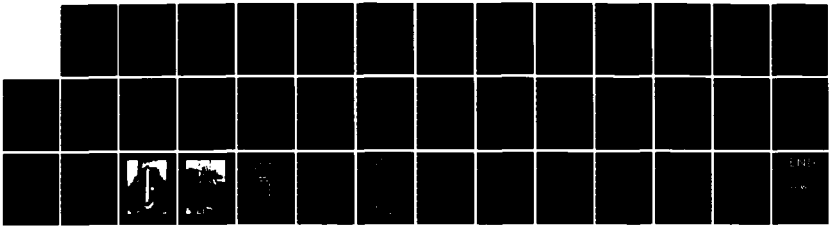

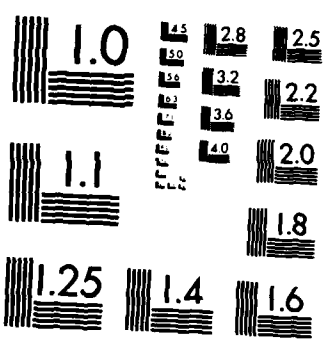

NRL Memorandum Report 5520

Fatigue Behavior of HY-130 Steel Weldments Containing Fabrication Discontinuities

S. J. GILL, J. A. HAUSER II, T. W. CROOKER,
B. J. KRUSE,* R. MENON,† AND C. D. LUNDIN†

Mechanics of Materials Branch
Material Science and Technology Division

**Duke Power Company*
Clover, SC 29710

†*University of Tennessee*
Knoxville, TN 37916

April 18, 1985

This research was supported by the Office of Naval Research
and the Welding Research Council.

NAVAL RESEARCH LABORATORY
Washington, D.C.

SECURITY CLASSIFICATION OF THIS PAGE

REPORT DOCUMENTATION PAGE

1a REPORT SECURITY CLASSIFICATION UNCLASSIFIED	1b RESTRICTIVE MARKINGS
2a SECURITY CLASSIFICATION AUTHORITY	3 DISTRIBUTION / AVAILABILITY OF REPORT
2b DECLASSIFICATION / DOWNGRADING SCHEDULE	Approved for public release; distribution unlimited.
4 PERFORMING ORGANIZATION REPORT NUMBER(S) NRL Memorandum Report 5520	5 MONITORING ORGANIZATION REPORT NUMBER(S)
6a NAME OF PERFORMING ORGANIZATION Naval Research Laboratory 6b OFFICE SYMBOL (If applicable) Code 6384	7a NAME OF MONITORING ORGANIZATION
6c ADDRESS (City, State, and ZIP Code) Washington, DC 20375-5000	7b ADDRESS (City, State, and ZIP Code)
8a NAME OF FUNDING / SPONSORING ORGANIZATION Office of Naval Research 8b OFFICE SYMBOL (If applicable)	9 PROCUREMENT INSTRUMENT IDENTIFICATION NUMBER
8c ADDRESS (City, State, and ZIP Code) Arlington, VA 22217	10 SOURCE OF FUNDING NUMBERS PROGRAM ELEMENT NO 61153N22 / PROJECT NO RR022-01-48 / TASK NO. / WORK UNIT ACCESSION NO DN080-024

11 TITLE (Include Security Classification)

Fatigue Behavior of HY-130 Steel Weldments Containing Fabrication Discontinuities

12 PERSONAL AUTHOR(S)

Gill, S.J., Hauser, J.A. II, Crooker, T.W., Kruse, B.J.,* Menon, R.,† and Lundin, C.D.†

13a TYPE OF REPORT	13b TIME COVERED	14 DATE OF REPORT (Year, Month, Day)	15 PAGE COUNT
Interim	FROM _____ TO _____	1985 April 18	40

16 SUPPLEMENTARY NOTATION

*Duke Power Company, Clover, SC 29710

†University of Tennessee, Knoxville, TN 37916

(Continues)

17 COSATI CODES		
FIELD	GROUP	SUB-GROUP

18 SUBJECT TERMS (Continue on reverse if necessary and identify by block number)

Base metal; Crack propagation; Crack initiation; Defects

(Continues)

19 ABSTRACT (Continue on reverse if necessary and identify by block number)

Fabrication discontinuities in weldments pose a serious engineering problem for structural applications involving cyclic loading. Often, the discovery of fabrication discontinuities through nondestructive inspection can pose a dilemma; if not properly repaired, failure can result from crack initiation and growth, however, if improperly repaired, post-repair discontinuities of even greater severity may result. Thus, a need exists for rational decision-making criteria to assess the mechanical severity of actual fabrication defects in weldments. This study was undertaken to explore the applicability of linear elastic fracture mechanics to characterize the fatigue behavior of high-strength steel weldments containing lack-of-penetration (LOP) and slag/lack-of-fusion (S/LOF) discontinuities. Full penetration, double-V butt welds with reinforcements removed were tested under zero-to-tension axial loading. Various filler metals and welding techniques were used. Both sound welds and welds containing discontinuities were cycled to failure. Whenever possible, cycles to crack initiation were

(Continues)

20 DISTRIBUTION / AVAILABILITY OF ABSTRACT	21 ABSTRACT SECURITY CLASSIFICATION
☒ UNCLASSIFIED/UNLIMITED ☐ SAME AS RPT ☐ DTIC USERS	UNCLASSIFIED
22a NAME OF RESPONSIBLE INDIVIDUAL S. J. Gill	22b TELEPHONE (Include Area Code) (202) 767-2947 / 22c OFFICE SYMBOL Code 6384

DD FORM 1473, 84 MAR 83 APR edition may be used until exhausted
All other editions are obsolete

SECURITY CLASSIFICATION OF THIS PAGE

16. SUPPLEMENTARY NOTATION (Continued)

This research was supported by the Office of Naval Research and the Welding Research Council.

18. SUBJECT TERMS (Continued)

Experimental data
Fatigue of materials
Fatigue tests
Fracture mechanics
High strength steels
Nickel chromium molybdenum steels
S-N diagrams
Weld defects
Weld metal

19. ABSTRACT (Continued)

estimated by strain gage measurements. The fracture mechanics approach was successful in correlating the fatigue lifetimes of specimens containing single LOP discontinuities of varying size. However, the fatigue behavior of specimens containing multiple S/LOF discontinuities proved to be much more complex and difficult to analyze.

CONTENTS

FATIGUE BEHAVIOR OF HY-130 STEEL WELDMENTS CONTAINING FABRICATION DISCONTINUITIES

S. J. Gill, J. A. Hauser II, T. W. Crooker,
B. J. Kruse,* R. Menon,** and C. D. Lundin**

Material Science and Technology Division
Naval Research Laboratory
Washington, DC 20375-5000

*Duke Power Company
Charlotte, NC
(formerly: Chemical, Metallurgical and Polymer Engineering
The University of Tennessee
Knoxville, TN 37916)

**Chemical, Metallurgical and Polymer Engineering
The University of Tennessee
Knoxville, TN 37916

INTRODUCTION

Nondestructive inspection (NDI) capabilities are steadily being improved. One result of this technological advancement is that fabrication discontinuities in weldments can now be more readily detected. This trend, in turn, places greater emphasis on the need for rational accept/reject criteria for discontinuities found in weldments.

In many instances, existing fabrication standards are based upon arbitrary discontinuity acceptance criteria. Frequently, such standards are derived largely from workmanship considerations. For situations where workmanship standards have a long history of satisfactory use, this is an acceptable approach. However, workmanship standards can also be costly and/or nonconservative when applied to the fabrication of failure-critical structures. Weld repairs to remove fabrication discontinuities can be costly to perform and, if not properly carried out, can introduce discontinuities (and residual stresses) more severe than the ones being removed. Weld repairs are often conducted under adverse conditions and can easily result in a product which is inferior to the original.

Manuscript approved January 14, 1985.

Thus, a strong need exists to develop rational criteria for discontinuity acceptance standards. This is often referred to as a fitness-for-purpose approach to discontinuity characterization. This approach has been applied in recent years to the development of several new codes and standards involving metal fatigue [1-4]. However, to date, this approach has yet to be developed for high-strength steels such as HY-130. Also, in some instances, the recent fitness-for-purpose criteria have been developed on a very conservative basis for application to situations where failure would incur very grave consequences, and thus may be inappropriate for general engineering application.

BACKGROUND

The present study was undertaken to explore the applicability of linear elastic fracture mechanics to characterize the fatigue behavior of HY-130 steel butt weldments containing internal lack-of-penetration (LOP) and slag/lack-of-fusion (S/LOF) discontinuities. For such welds total fatigue life can be divided into a period of crack initiation, in which the discontinuity does not enlarge perceptibly, and a subsequent period of crack propagation in which a crack originating at the flaw enlarges until fracture occurs. Crack initiation and crack propagation both play important roles in the overall fatigue failure process. The present study is aimed at understanding the relative importance of each phase of fatigue failure for high-strength steel weldments containing internal discontinuities, to assess the ability of fracture mechanics in analyzing both phases, and to characterize the effects of various discontinuity sizes and shapes on fatigue life.

MATERIALS AND SPECIMEN PREPARATION

The test specimens used in this study were fabricated from 25-mm (1-in.) thick HY-130 steel plate material joined by various weld metals, including 7018, 9018, 11018 and 14018. The chemistry and mechanical properties of the HY-130 plate material are given in Tables 1 and 2. Chemistries of the various weld metals are given in Table 3.

Full-penetration, double-V groove butt welds were used to fabricate the axially-loaded fatigue specimens, Figure 1. Typical welding and post weld heat treatment conditions for the fabrication of the test specimens, using the shielded metal-arc (SMA) process, are listed in Table 4. Several types of welds were prepared and studied. Discontinuity-free sound welds and welds containing LOP discontinuities were prepared using 14018 weld metal under contract by the Southwest Research Institute. Specimens containing S/LOF discontinuities using a variety of weld metals were prepared by the University of Tennessee under a joint cooperative research program. Welding procedures were in general agreement with Navy standards for HY-130 fabrication [5]. However, the intentional formation of specific discontinuities in welds is an unusual and highly selective procedure. LOP discontinuities were formed by butting large land areas which were left unjoined in subsequent weld passes. S/LOF discontinuities were formed by entrapping slag deposits. Both procedures were accomplished using multipass manual methods.

After welding, reinforcements were ground smooth to assure that internal discontinuity behavior would control the fatigue failure process. Also, the

weld region was reduced slightly in width to further assure that fatigue failures would initiate in the desired location. Following preparation, all specimens were examined using radiographic inspection to determine the features of the internal discontinuities. The axial loading applied to the specimens assured that the cyclic stresses were uniform across the test section of the welds.

TEST PROCEDURES

The fatigue specimens were tested under constant-stress-amplitude zero-to-tension cyclic loading, with the load ratio $R = P_{min}/P_{max} = 0$. The specimens were loaded in a 2.7-MN (600,000-lb.) capacity closed-loop servo-hydraulic fatigue machine equipped with large hydraulic squeeze grips, so that the plate samples could be gripped directly without requiring any special machining or preparation.

All specimens were tested to complete fracture. However, the tests were monitored periodically to determine the onset of internal fatigue cracking. This was accomplished by placing strain gages on the specimen test section. Strain gage readings provided a sensitive indication of the point in the fatigue life where significant enlargement of internal defects began to occur. This point is regarded as the fatigue crack initiation life.

The post-failure fracture surfaces of each specimen were examined to various degrees, depending upon the particular specimen and its fatigue behavior. Initial discontinuity sizes were carefully measured and recorded for use in the fracture mechanics analysis of the fatigue life data. Crack initiation sites were noted and micro-fracture modes were determined.

RESULTS AND ANALYSIS

Fatigue Life Data

The raw fatigue life data summarized in Table 5 and are plotted in Figures 2 and 3, which are semilogarithmic plots of stress amplitude (S) versus cycles-to-failure (N_f) and cycles-to-initiation (N_i), respectively. These plots include data from 10 sound weld specimens, 11 specimens containing LOP discontinuities, and 18 specimens containing S/LOF discontinuities from this investigation. In addition, selected data from a previous investigation by Lawrence and Radziminski [6] are also included for purposes of comparison.

The fatigue life data shown in Figures 2 and 3 represent a broad range of stress levels and fatigue lifetimes. Stress amplitudes vary from 276 to 827 MPa (40 to 120 ksi), approximately 30 to 90 percent of nominal yield strength, and the fatigue lifetimes vary from approximately 2×10^2 to 4×10^5 cycles. Most of these data fall within the fatigue life range of what is generally considered to be low-cycle fatigue, i.e., less than 10^5 cycles to failure. However, the high-strength HY-130 steel studied in this investigation did not develop the cyclic plastic deformation normally associated with low-cycle fatigue testing [7].

The data in Figures 2 and 3 indicate a very broad spectrum of fatigue lifetimes as a function of stress amplitude and discontinuity character-

istics. The fatigue lifetimes, either N_f or N_i, can vary by as much as two orders of magnitude at a given stress level depending upon discontinuity severity. Thus, it is apparent that discontinuity characteristics play a crucial role in the fatigue behavior of HY-130 steel weldments, and that fatigue life is a function of both stress amplitude and discontinuity characterization parameters.

The relationship between N_f and N_i for the sound welds is shown in Figure 4. This is consistent with previous observations that crack initiation constitutes a larger percentage of total fatigue life as fatigue lifetimes become longer [8].

Fracture Mechanics Methodology

Linear elastic fracture mechanics provides a means of quantitatively assessing the behavior of cracks under stress [8]. Fracture mechanics procedures were used in this investigation to analyze two aspects of the fatigue behavior of the HY-130 weldments: (1) to provide a comprehensive parameter which incorporates stress level, flaw size and flaw shape in order to correlate initial as-fabricated discontinuities with fatigue life and (2) to provide a description of crack growth emanating from fabrication discontinuities. The fracture mechanics parameter used in both instances is the crack-tip stress-intensity factor, K_I [8]. K_I incorporates both stress and flaw size terms and is proportional to the product of nominal stress and the square root of flaw size,

$$K_I = C\sigma\sqrt{\pi a}, \qquad (1)$$

where C is a constant which is a function of specimen type and crack geometry, σ is nominal stress, a is flaw size and the subscript I denotes the opening mode of crack displacement. For the purposes of this report, it will be assumed that all reference to K values will imply Mode I conditions.

The analysis of both aspects of fatigue behavior by fracture mechanics procedures was dependent upon the ability to assign an effective K value to weld discontinuities. Herein lies the central focus of this investigation. Handbook stress-intensity factor solutions have been derived for infinitely sharp planar cracks of regular geometric proportions. In most instances, weld discontinuities fail to meet these criteria and the engineering application of fracture mechanics to defect characterization necessarily involves approximation and improvisation. Details of these analytical procedures are described separately for LOP and S/LOF discontinuities in subsequent sections of this report.

The general fracture mechanics methodology employed was to assign an initial K value to as-fabricated discontinuities. Initial K values were used in two ways: (1) to correlate with corresponding N_i and N_f data in an attempt to provide a degree of quantitative discontinuity characterization lacking in the S-N plots of Figures 2 and 3, and (2) to use in a crack growth rate analysis of the number of cycles spent in crack propagation ($N_f - N_i$).

The calculation of the number of cycles spent in crack propagation was performed by well known procedures, as follows. The Paris law [8] was used to describe the average per cycle incremental crack growth advance by the following equation.

$$\frac{da}{dN} = C(\Delta K)^n \tag{2}$$

where:

$\frac{da}{dN}$ = rate of crack advance per cycle

C = material constant

n = material constant

ΔK = range of stress-intensity factor = $K_{max} - K_{min}$

Fatigue life spent in crack propagation may be obtained by integrating the Paris equation,

$$N = \int_{a_o}^{a_f} \frac{1}{C(\Delta K)^n} da \tag{3}$$

where:

N = cycles spent in advancing the crack from a_o to a_f

a_o = initial half crack size (defect dimension in direction of subsequent crack growth)

a_f = final half crack size.

In those cases where the integration of equation (3) is difficult a finite difference technique can be used and the integration performed numerically with the aid of a computer.
Thus,

$$N = \sum_{a_o}^{a_f} \frac{\Delta a}{C(\Delta K)^n} \tag{4}$$

where:

Δa = small finite advance of the crack.

For each welded fatigue specimen studied in this investigation, measurements were made of the planar dimensions of the initial weld discontinuity which generated the largest final fatigue crack, i.e., the dominant crack. These dimensions were then used to generate an effective initial discontinuity represented by a fully-embedded elliptical discontinuity, for which fracture mechanics solutions are readily obtainable [9]. The critical dimensions of elliptical discontinuities are the minimum and maximum radii values. For the purposes of this investigation, post-failure measurements were made of the planar dimensions of initial discontinuities at 1-mm (0.040-in.) intervals to establish their size.

Typically, the discontinuities studied in this investigation were either roughly rectangular (LOP) or irregular and elongated (S/LOF). Examples are shown in Figures 5 and 6. Numerous questions arise in equating such fabrication discontinuities to solutions for elliptical discontinuities. One such approach has been formalized in the ASME Section XI Boiler and Pressure Vessel Code [1]. There, the procedure is an innately conservative one; i.e., to define the effective fracture mechanics discontinuity as an ellipse which surrounds or fully encloses the fabrication discontinuities. However, for the purposes of the present analysis, more consistent results were obtained by choosing elliptical geometries which best fit within the major dimensions of the fabrication discontinuities. This latter procedure produced

analytical results which gave much less scatter, as shown in Table 6.

It is recognized that discontinuity shape, as well as size, is an important variable in analyzing crack growth. For the purposes of this study, it was assumed that during crack growth both the major and minor radii of the fully-embedded elliptical discontinuities varied as a function of the stress-intensity factor.

Fatigue life calculations using Equation 4 were made using the following Paris equation parameter values.

$$C = 8.54 \times 10^{-7} \text{ (m/cycle)/(MPa}\sqrt{\text{m}})^n$$
$$= 4.13 \times 10^{-9} \text{ (in./cycle)/(ksi}\sqrt{\text{in.}})^n$$
$$n = 2.176$$

These values were obtained from previous NRL studies on HY-130 steels [10].

In applying Equation 4, a_o was taken to be half the maximum through-thickness dimension of the fabrication discontinuity and a_f was taken to be the half thickness, t, of the plate material. However, there are two valid arguments for ending the summation even before the internal discontinuity has reached the surface. One relates to net section stress and the other relates to fracture toughness. Accordingly, the computer program which performed the summation was written such that the summation would be ended if the net section stress exceeded 1034 MPa (150 ksi) or the maximum stress intensity exceeded 180 MPa$\sqrt{\text{m}}$ (150 ksi$\sqrt{\text{in.}}$). It is also recognized that, mathematically, a_o exerts a much greater influence on cycles to failure than does a_f. Thus, efforts to characterize initial discontinuity severity have a greater potential to influence fatigue life estimates than do final failure criteria.

Finally, fracture mechanics methodology was used so that data from specimens which lacked intentional initial discontinuities could also be included in summary plots of initial K versus N_1 and N_f. In conducting this analysis, it was assumed that the supposedly unflawed specimens behaved as if some finite initial discontinuity did, in fact, exist. The equivalent initial discontinuity size of the sound-weld specimens could then be defined as that which places the initial K versus N_f data on the same line as that which describes the flawed specimens.

This was done by first fitting an equation to the initial K versus N_f data for the LOP specimens, as follows.

$$\text{initial } K = m_1 \log_{10} N + b_1$$

Similarly, a line was fit to all the S-N data for sound weld specimens and was described by an equation of the following form

$$S = m_2 \log_{10} N + b_2$$

Letting initial $K = S\sqrt{a_{eq}}$, it was possible to estimate a_{eq} from

$$\sqrt{a_{eq}} = \frac{m_1 \log_{10} N + b_1}{m_2 \log_{10} N + b_2}$$

The resulting values of a_{eq} are tabulated in Table 7. Two results are apparent from these data. First, there is about a 2:1 variation in a_{eq} depending upon whether the initial K values are calculated with the ellipse lying inside or outside fabrication discontinuities. Second, regardless of which assumption is made, a_{eq} values exhibit a good measure of consistency. Using the preferred method of placing the ellipse inside the fabrication discontinuities, a_{eq} averages out to be on the order of 2.5 mm (0.10 in.) for the sound-weld specimens.

Lack-of-Penetration Discontinuity Analysis

The lack-of-penetration discontinuities were essentially rectangular and were either fully embedded or full-width internal discontinuities. They were approximated by the following two stress-intensity factor solutions. The first is for a fully-embedded elliptical discontinuity and the second is for a rectangular through discontinuity.

A model for a discontinuity in a weld, an embedded elliptical discontinuity in a plate, is shown in Figure 7. The stress intensity for a zero-to-tension stress condition (stress perpendicular to the plane of the crack) as defined in Reference 11 would be:

$$K_I = S\sqrt{\pi\frac{a}{Q}}\,F_e\left(\frac{a}{c}, \frac{a}{t}, \frac{c}{b}, \phi\right) \tag{5}$$

for $0 \leq a/c \leq \infty$, $c/b < 0.5$, and $-\pi \leq \phi \leq \pi$ provided that a/t satisfies:

$$\begin{aligned} &\frac{a}{t} < 1.25\left(\frac{a}{c} + 0.6\right) && \text{for } 0 \leq \frac{a}{c} \leq 0.2 \\ &\frac{a}{t} \leq 1 && \text{for } 0.2 \leq \frac{a}{c} < \infty \end{aligned} \tag{6}$$

where Q is the shape factor for an ellipse and is given by the square of the complete elliptic integral of the second kind. The width (b) and length (h) of the plate were taken to be large enough so that they would have a negligible effect on stress intensity. The boundary correction, F, accounts for the influence of various boundaries and is a function of crack depth, crack length, hole radius (where applicable), plate thickness, and the parametric angle of the ellipse. Figure 8 shows the coordinate system used to define the parametric angle.

Very useful empirical expressions for Q have been developed. The expressions are, for $a/c \leq 1.0$, which was the case for all of the specimens examined,

$$Q = 1 + 1.464\left(\frac{a}{c}\right)^{1.65} \tag{7}$$

The maximum error in the stress intensity factor caused by using these equations for Q was about 0.13 percent for all values of a/c.

The function F_e accounts for the influence of crack shape (a/c), crack size (a/t), finite width (c/b), and angular location (ϕ), and was chosen as

$$F_e = \left[M_1 + M_2 \left(\frac{a}{t}\right)^2 + M_3 \left(\frac{a}{t}\right)^4 \right] g\, f_\phi\, f_w \tag{8}$$

The term in brackets gives the boundary-correction factors at $\phi = \pi/2$ (where $g = f_\phi = 1$). The function f_ϕ was taken from the exact solution for an embedded elliptical discontinuity in an infinite solid and f_w is a finite-width correction factor. The function g is a fine-tuning curve-fitting function. For $a/c \leq 1$:

$$M_1 = 1 \tag{9}$$

$$M_2 = \frac{0.05}{0.11 + \left(\frac{a}{c}\right)^{3/2}} \tag{10}$$

$$M_3 = \frac{0.29}{0.23 + \left(\frac{a}{c}\right)^{3/2}} \tag{11}$$

$$g = 1 - \frac{\left(\frac{a}{t}\right)^4}{1 + 4\left(\frac{a}{c}\right)} \left| \cos \phi \right| \tag{12}$$

$$f_\phi = \left[\left(\frac{a}{c}\right)^2 \cos^2 \phi + \sin^2 \phi \right]^{1/4} \tag{13}$$

The finite-width correction, f_w, was

$$f_w = \left[\sec \left(\frac{\pi c}{2b} \sqrt{\frac{a}{t}} \right) \right]^{1/2} \tag{14}$$

for $c/b < 0.5$. (Note that for the embedded discontinuity, t is defined as one-half of the full plate thickness.)

A second model, that of a through discontinuity in a body which is finite in the direction of crack advance, is shown in Figure 9. This model describes a situation which arises intentionally when partial-penetration welds are specified to obtain cost savings over full-penetration welds. The range of stress intensity for a zero-to-tension stress situation can be expressed according to Reference 12 as:

$$\Delta K = \sigma \sqrt{\pi a} \left(\sec \frac{\pi a}{2b} \right)^{1/2}, \quad 0 \leq a \leq 0.8b \tag{15}$$

where b = plate half thickness.

The initial K versus N_f and N_i data are plotted in Figures 10 and 11, respectively. The data show a good agreement between the lifetimes of the welds containing LOP discontinuities and the models used. Compared with the data in Figures 2 and 3, the use of a fracture mechanics approach has successfully normalized the data.

Slag/Lack-of-Fusion Discontinuities Analysis

The slag/lack-of-fusion discontinuities were roughly elliptical and were fully embedded, so they were described by the solution for a fully-embedded elliptical discontinuity given in the preceding section. The initial K versus N_f and N_i data are plotted in figures 12 and 13, respectively. The data show only a low correlation between lifetimes of welds containing multiple S/LOF discontinuities and the initial K values calculated by ignoring all S/LOF discontinuities except the one yielding the largest fatigue crack.

DISCUSSION

The fracture mechanics analysis methods employed in this investigation were two-dimensional; i.e., they dealt only with the planar dimensions of the discontinuities, length and width in the cross-sectional plane. Thus, discontinuity acuity or sharpness was not taken into consideration. For the fatigue behavior of the LOP discontinuities, this appears to have been a reasonably successful approach. The data in Figures 10 and 11, initial K versus N_f and N_i, respectively, for the LOP specimens, are nicely normalized with respect to stress level and discontinuity size. LOP discontinuities are categorized in the British Standards Institution document on discontinuty assessment for fatigue as being "planar" or crack-like [2], and thus should be largely amenable to a straightforward fracture mechanics approach.

However, it should be pointed out that some degree of conservatism is built into the assumptions underlying the approach used in the plots shown in Figures 10 and 11. Despite the planar nature of the LOP discontinuities, they are not fully crack-like and some period of crack initiation life was observed in most instances. This is illustrated in Figure 14, which is a plot of observed cycles-to-failure versus calculated cycles-to-failure using the crack growth rate methodology described earlier. Except for specimens which failed in very short fatigue lifetimes, the trend is for actual fatigue life to exceed calculated fatigue life; thus suggesting that even planar LOP discontinuities are not, in fact, truly crack-like with regard to their fatigue behavior.

The successful normalization of the LOP data is not matched for the LOF data, Figures 12 and 13. Here, unlike the LOP specimens, multiple initial discontinuities existed in each specimen. In undertaking a fracture mechanics analysis of the data, attention was focused on selecting the initial discontinuities which appeared to initiate crack growth first, and thus produced the largest fatigue crack at failure. Obviously, something other than this unrefined approach is needed. Only the broadest correlation trend between initial K and N_f and N_i is apparent in the data shown in Figures 12 and 13.

Several complicating factors affect the S/LOF data. The S/LOF

discontinuities were formed by intentionally leaving entrapped slag in the welds. The British Standards Institution document categorizes slag discontinuities as being "non-planar" [2], and thus something less severe than crack-like. Post-failure examination of the S/LOF specimens revealed that, in many instances, the largest initial slag discontinuities did not lead most quickly to failure. Discontinuity acuity and/or the surrounding residual stress field played more important roles than discontinuity size, per se. Obviously, a great deal more needs to be learned before the fatigue behavior of multiple S/LOF discontinuities can be predicted with confidence and accuracy.

Finally, the S/LOF specimens tested consisted of a mixture of weld metals (7018, 9018, 11018 and 14018) of varying yield strengths approximately 480 to 960 MPa (70 to 140 ksi). Amongst these were specimens tested in the as-welded (AW) and post-weld heat-treated (PWHT) conditions. Figure 15 shows stress-amplitude versus N_f data for these specimens. These limited data do not suggest any significant effect of strength level, per se, on fatigue life. This is as expected for the fatigue life regime involved ($N_f < 10^5$ cycles to failure). However, the PWHT does appear to impart significant benefits to fatigue life, thus suggesting that residual tensile stress plays an important role in fatigue crack initiation at S/LOF discontinuities.

SUMMARY AND CONCLUSIONS

Butt-welded HY-130 steel specimens containing internal lack-of-penetration (LOP) and slag/lack-of-fusion (S/LOF) discontinuities were cycled to failure at nominal stress levels from 276 to 827 MPa (40 to 120 ksi) and resulting fatigue lifetimes between 10^2 and 10^6 cycles. Strain-gage instrumentation was employed to estimate the point of crack initiation during fatigue cycling. Attempts were made to analyze fatigue behavior on the basis of linear elastic fracture mechanics parameters. The following conclusions were reached as a result of this investigation.

- For specimens containing single planar LOP discontinuities of varying sizes, a good correlation was obtained between the initial stress-intensity (K) and cycles-to-failure (N_f) and cycles-to-initiation (N_i). The rectangular LOP discontinuities were most successfully approximated for fracture mechanics analysis purposes by elliptical discontinuity solutions, for ellipses lying within the boundaries of the rectangular discontinuities. This approach embodies an inherent degree of conservatism because, even for the planar LOP discontinuities, a significant period of crack initiation occured, except for very short fatigue lifetimes.

- For specimens containing multiple non-planar S/LOF discontinuities, a satisfactory correlation between initial K and N_f or N_i could not be readily obtained. The effects of discontinuity acuity and surrounding residual stress fields appear to exert a greater influence than discontinuity size, per se. Additional study is needed before reliable engineering criteria relating to S/LOF discontinuity behavior in fatigue can be developed.

- For specimens containing S/LOF discontinuities prepared with a variety of weld metals of varying yield strengths, strength level, per se, did

not exhibit any tangible influence on fatigue life. However, post-weld heat-treatment did have significant beneficial effects on fatigue life.

ACKNOWLEGDMENTS

Financial support for this research was provided by the Office of Naval Research and the Welding Research Council. Experimental assistance was provided by M. L. Cigledy, G. W. Jackson and J. L. Berman.

REFERENCES

[1] ASME Boiler and Pressure Vessel Code, Section XI, "Rules for Inservice Inspection of Nuclear Reactor Coolant Systems," American Society of Mechanical Engineers, 1980.

[2] PD 6493: 1980: "Guidance on Some Methods for the Derivation of Acceptance Levels for Defects in Fusion Welded Joints," British Standards Institution.

[3] R. P. Reed, H. I. McHenry and M. B. Kasen, "A Fracture Mechanics Evaluation of Flaws in Pipeline Girth Welds," Welding Research Council Bulletin 245 (1979).

[4] W. S. Pellini, Guidelines for Fracture-Safe and Fatigue-Reliable Design of Steel Structures (The Welding Institute, Cambridge, England, 1983).

[5] Military Standard, "Fabrication, Welding and Inspection of HY-130 Submarine Hulls," MIL-STD-1681 (SH), 29 March 1976.

[6] F. V. Lawrence, Jr. and J. B. Radziminski, "Fatigue Crack Initiation and Propagation in High-Yield-Strength Steel Weld Metal," Welding Journal, Research Supplement 49, 445-S - 452-S (1970).

[7] E 513-74, Standard Definitions of Terms Relating to Constant-Amplitude Low-Cycle Fatigue Testing, 1983 Annual Book of ASTM Standards, 03.01, (American Society for Testing and Materials, Philadelphia, Pa., 1983), pp. 586-587.

[8] S. T. Rolfe and J. M. Barsom, Fracture and Fatigue Control in Structures (Prentice-Hall, Englewood Cliffs, New Jersey, 1977).

[9] R. J. Pick, "Stress Intensity Factors: Their Prediction and Use in Design," Canadian Metallurgical Quarterly, 19, 34-44, (1980).

[10] A. M. Sullivan and T. W. Crooker, "Analysis of Fatigue-Crack Growth in a High-Strength Steel - I: Stress Level and Stress Ratio Effects at Constant Amplitude," ASME Transactions, Ser. J., Journal of Pressure Vessel Technology, 98, 179-184 (1976).

[11] J. C. Newman, and I. S. Raju, "Stress-Intensity Factor Equations for Cracks in Three-Dimensional Finite Bodies," Fracture Mechanics: Fourteenth Symposium - Volume I: Theory and Analysis, ASTM STP 791,

J. C. Lewis and G. Sines, Eds. (American Society for Testing and Materials, Philadelphia, Pa., 1983), pp. I-238 - I-265.

[12] C. E. Feddersen, Discussion to Plane Strain Crack Toughness Testing of High Strength Metallic Materials, by Brown, W. F., and Srawley, J. E., ASTM STP 410. (American Society for Testing and Materials, Philadelphia, Pa., 1966), pp. 77-79.

TABLE 1- CHEMICAL COMPOSITION OF BASE METAL AND WELD METAL

ELEMENT	WEIGHT PER CENT	
	BASE METAL	WELD METAL (E 14018)
CARBON	0.07	0.11
MANGANESE	0.72	0.92
PHOSPHORUS	0.009	0.005
SULFUR	0.003	----
SILICON	0.29	0.20
NICKEL	4.95	3.97
CHROMIUM	0.48	0.53
MOLYBDENUM	0.47	0.66
VANADIUM	0.07	0.08
TITANIUM	0.005	----

TABLE 2- MECHANICAL PROPERTIES

SOURCE	REGION	YIELD STRENGTH MPa	YIELD STRENGTH (ksi)	ULTIMATE STRENGTH MPa	ULTIMATE STRENGTH (ksi)	ELONGATION %	REDUCTION IN AREA %	CHARPY V NOTCH J	CHARPY V NOTCH (ft-lbs)	CHARPY V NOTCH °C (°F)
MANUFACTURER	BASE	962	(139.5)	990	(143.6)	19	70.8	210 *	(155) *	21 (70)
		948	(137.5)	973	(141.1)	20	71.8	193 *	(142) *	21 (70)
								198 *	(146) *	21 (70)
								214 **	(158) **	21 (70)
								201 **	(148) **	21 (70)
								199 **	(147) **	21 (70)
								156 *	(115) *	−18 (0)
								172 *	(127) *	−18 (0)
								164 *	(121) *	−18 (0)
								187 **	(138) **	−18 (0)
								187 **	(138) **	−18 (0)
								201 **	(148) **	−18 (0)
FABRICATOR	BASE							145***	(107)***	−7 (20)
	HAZ							118***	(87)***	−7 (20)
	WELD							106***	(78)***	−7 (20)
	TRANS-VERSE WELD			954	(138.3)					
				929	(134.8)					

* TRANSVERSE ** LONGITUDINAL *** AVERAGE OF THREE TESTS

TABLE 3- CHEMICAL COMPOSITION OF ELECTRODES USED

MANUFACTURER	AIRCO	AIRCO	AIRCO	TELEDYNE McKAY
ELECTRODE DESIGNATION	7018	9018B3	11018M	14018
HEAT NUMBER	NA	NA	NA	645K566
ELECTRODE TYPE	COVERED	COVERED	COVERED	COVERED
ELECTRODE *DIAMETER, mm (in.)*	3 (1/8)	3 (1/8)	3 (1/8)	3 (1/8) 4 (5/32)
ELEMENT	CHEMICAL COMPOSITION, %			
CARBON	0.04	0.034	0.04	0.057
MANGANESE	0.65	0.53	1.60	0.96
PHOSPHORUS	0.011	0.013	0.012	0.005
SULFUR	0.013	0.014	0.016	0.007
SILICON	0.55	0.66	0.40	0.21
NICKEL			1.80	3.57
CHROMIUM		2.40	0.25	0.50
MOLYBDENUM		0.98	0.42	0.71
VANADIUM				0.01

TABLE 4- PROCEDURES FOR PREPARATION OF BUTT WELDS

WELDING PARAMETER	ELECTRODE			
	7018	901883	11018M	14018
WELDING PROCESS	SMA (MANUAL)	SMA (MANUAL)	SMA (MANUAL)	SMA (MANUAL)
ELECTRODE DIAMETER, mm. (in)	3 (1/8)	3 (1/8)	3 (1/8)	3 (1/8) 4 (5/32)
CURRENT, AMPERES	120-140	120-140	120-140	
POLARITY	DC REVERSED POLARITY	DC REVERSED POLARITY	DC REVERSED POLARITY	DC REVERSED POLARITY
VOLTAGE, VOLTS	21-25	21-25	21-25	
PREHEAT AND INTERPASS TEMPERATURE °C (°F)	107-149 (225-300)	107-149 (225-300)	107-149 (225-300)	107-149 (225-300)
ARC TRAVEL SPEED m/min (in./min)	203-305 (8-12)	203-305 (8-12)	203-305 (8-12)	203-406 (8-16)
MAXIMUM HEAT INPUT MJ/m. (kJ/in.)	1.03 (26.25)	1.03 (26.25)	1.03 (26.25)	1.77 (45)
SHIELDING GAS	NONE	NONE	NONE	NONE
JOINT GEOMETRY	90° DOUBLE V	90° DOUBLE V	90° DOUBLE V	90° DOUBLE V
DISCONTINUITY TYPE	S/LOF	S/LOF	S/LOF	LOP, S/LOF
POST WELD HEAT TREATMENT	621°C (1150°F) FOR 1 hr., AIR COOL	690°C (1275°F) FOR 1 hr., AIR COOL	566°C (1050°F) FOR 1 hr., AIR COOL	NONE

TABLE 5- RESULTS OF FATIGUE TESTS

ID	a mm.	b mm.	c mm.	t mm.	DELTA S MPa	N_i CYCLES	N_f CYCLES	DISCONTIN-UITY TYPE
1	0	35.6	0	12.8	552	27000	59417	NONE
2	0	37.3	0	12.8	552	*	33119	NONE
3	0	39.3	0	12.7	690	9750	24793	NONE
4	2.1	36.8	36.8	12.7	552	5650	9453	LOP
5	0	36.8	0	12.7	690	5200	13065	NONE
7	2.1	37.2	37.2	12.7	552	3750	10255	LOP
8	2	36.2	8.1	12.5	690	1600	5750	LOP
9	2.1	37.8	37.8	13	414	9750	19900	LOP
11	1.6	34.1	19.9	12.3	414	10750	35827	LOP
12	0	36.6	0	12.7	414	62500	113949	NONE
13	0	36.3	0	12.6	276	261000	357033	NONE
14	2.2	36.5	21.4	12.7	690	*	3754	LOP
15	1.9	37.5	7.3	12.8	552	1000	21225	LOP
16	0	36.7	0	12.7	827	*	10000	NONE
17	0	34.9	0	12.7	827	*	13509	NONE
18	0	35.6	0	13.3	690	6500	28011	NONE
19	0	36.2	0	12.9	414	70000	104959	NONE
20	2.1	37.4	8.2	12.6	414	13500	50500	LOP
21	1.9	36.4	20.2	12.6	552	1000	12937	LOP
22	2	37.1	37.1	12.9	690	375	3459	LOP
23	2.1	37.3	7.6	12.7	552	*	23389	LOP
ND-20	.7	50.8	3.8	12.7	345	5000	36000	LOP
ND-12	.5	50.8	6.6	12.7	345	175000	219200	LOP
NA-1	0	31.7	0	12.7	552	*	64200	NONE
NA-2	0	31.7	0	12.7	552	*	60900	NONE
NC-13	0	31.7	0	12.7	552	*	59800	NONE
NA-5	0	31.7	0	12.7	552	*	51100	NONE
NC-14	0	31.7	0	12.7	552	*	50500	NONE

* NOT MEASURED

TABLE 5- RESULTS OF FATIGUE TESTS (Cont'd)

ID	a mm.	b mm.	c mm.	t mm.	DELTA S MPa	N_i CYCLES	N_f CYCLES	DISCONTIN-UITY TYPE
7018N1	.4	41.2	6.7	12.9	414	4500	8557	S/LOF
7018N2	1	42	4	12.9	448	*	6300	S/LOF
7018N3	0	40.5	0	12.7	448	*	107392	NONE
7018N4	.6	42.8	22.3	12.7	379	15000	73664	S/LOF
9018N1	.6	41.6	3.6	12.9	579	250	2003	S/LOF
9018N2	.2	41.4	6.8	12.9	345	20000	56800	S/LOF
9018N3	0	37.4	0	12.9	345	*	271500	NONE
9018N4	.5	38.4	10.4	12.9	483	500	16804	S/LOF
11018N1	.4	42.6	5.3	12.9	579	1250	13627	S/LOF
11018N2	.1	39.6	9.2	12.9	379	6250	21500	S/LOF
11018N3	.6	44.2	6.2	12.7	579	3750	18000	S/LOF
11018N4	.6	42.6	14.8	13	345	55000	82400	S/LOF
14018N1	.4	41.9	32.8	12.7	552	500	1317	S/LOF
14018N2	1	39.5	21.2	13	552	*	1849	S/LOF
14018N3	1	41.9	21.2	13	690	*	1096	S/LOF
14018N5	1.3	41.3	8.6	12.8	414	*	5896	S/LOF
14018N6	1.3	42.5	22.7	13	276	20000	65472	S/LOF
14018N7	3	44	20.3	12.9	414	*	7531	S/LOF
ND-18	.6	50.8	6.9	12.7	345	60000	83800	S/LOF
ND-17	1.2	50.8	12	12.7	345	27500	71300	S/LOF
ND-19	.8	50.8	8.8	12.7	345	17500	52000	S/LOF
ND-16	.2	31.7	3.8	12.7	552	*	6200	S/LOF
ND-46	.6	31.7	2.2	12.7	552	38000	42850	S/LOF
ND-47	.6	31.7	.7	12.7	552	5450	10400	S/LOF
ND-45	1	31.7	2.7	12.7	552	1020	6750	S/LOF
ND-38	.5	31.7	.7	12.7	552	500	5700	S/LOF
NE-8	.2	31.7	5.5	12.7	552	1750	4970	S/LOF
NE-7	1.1	31.7	1.5	12.7	552	250	2870	S/LOF
NE-12	1	31.7	.6	12.7	552	1500	4400	S/LOF

* NOT MEASURED

TABLE 6- GOODNESS OF FIT FOR N VERSUS $K_{INITIAL}$ DATA

FLAW	N	LOCATION OF ASSUMED INITIAL ELLIPSE RELATIVE TO DISCONTINUITY					
		INSIDE			OUTSIDE		
		CORRELATION COEFFICIENT	COEFFICIENT OF DETER-MINATION	STANDARD ERROR OF THE ESTIMATE	CORRELATION COEFFICIENT	COEFFICIENT OF DETER-MINATION	STANDARD ERROR OF THE ESTIMATE
LOP	N_i	0.78177	0.61117	8.1508	0.61168	0.37415	13.092
	N_f	0.92507	0.85575	5.0519	0.60812	0.36981	12.833
	N_f-N_p	0.96361	0.92855	2.9873	0.50735	0.25741	13.754
S/LOF	N_i	0.40211	0.16169	4.3575	0.23000	0.05290	7.8116
	N_f	0.49873	0.24873	6.2275	0.13254	0.01756	20.099
	N_f-N_p	0.45410	0.20621	2.9732	0.28292	0.08004	29.119

TABLE 7- EFFECTIVE INITIAL FLAW SIZES FOR UNFLAWED SPECIMENS

	LOCATION OF ASSUMED INITIAL ELLIPSE RELATIVE TO DISCONTINUITY							
	INSIDE				OUTSIDE			
	$N=N_i$		$N=N_f$		$N=N_i$		$N=N_f$	
	EFFECTIVE INITIAL FLAW SIZE							
	mm	in	mm	in	mm	in	mm	in
1	2.395	0.09428	2.289	0.09013	4.211	0.1658	4.831	0.1902
2			2.654	0.1045			4.615	0.1817
3	2.516	0.09904	2.807	0.1105	3.988	0.1570	4.531	0.1784
5			3.091	0.1217	3.886	0.1530	4.384	0.1726
12	2.251	0.08861	1.760	0.06929	4.496	0.1770	5.184	0.2041
13	1.802	0.07095	0.424	0.01669	5.509	0.2169	6.574	0.2588
16			3.193	0.1257			4.333	0.1706
17			3.079	0.1212			4.389	0.1728
18	2.553	0.1005	2.743	0.1080	3.919	0.1543	4.567	0.1798
19	2.227	0.08766	1.834	0.0722	4.544	0.1789	5.131	0.2020
NA-1			2.234	0.08795			4.864	0.1915
NA-2			2.272	0.08944			4.841	0.1906
NC-13			2.285	0.08995			4.834	0.1903
NA-5			2.392	0.09418			4.768	0.1877
NC-14			2.400	0.09449			4.763	0.1875

EFFECTIVE INITIAL FLAW SIZE

$$A_{EFFECTIVE} = \left[\frac{m_1 \log_{10} N + b_1}{m_2 \log_{10} N + b_2}\right]^2$$

WHERE $K_{INITIAL}$ VERSUS N DATA FOR LOP SPECIMENS IS DESCRIBED BY

$$K_{INITIAL} = m_1 \log_{10} N + b_1$$

AND S VERSUS N DATA FOR UNFLAWED SPECIMENS IS DESCRIBED BY

$$S = m \log_{10} N + b_2$$

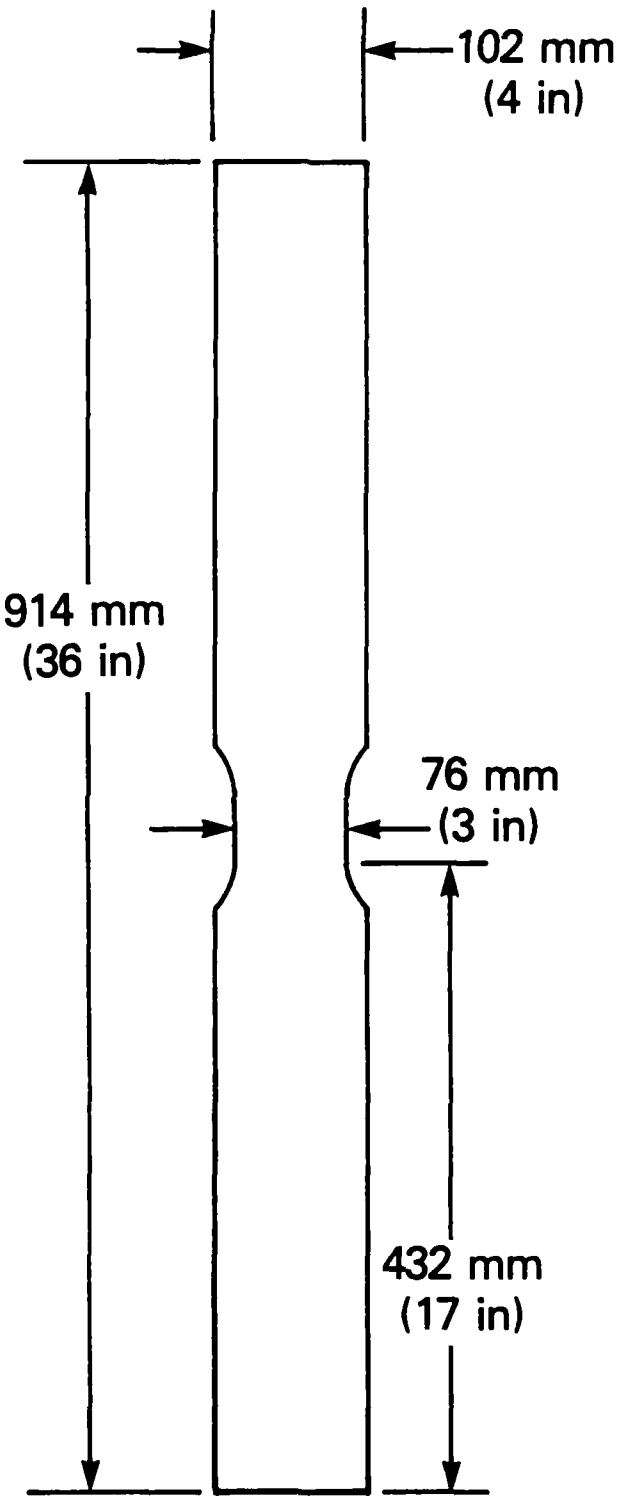

Fig. 1 - Welded fatigue test specimen.

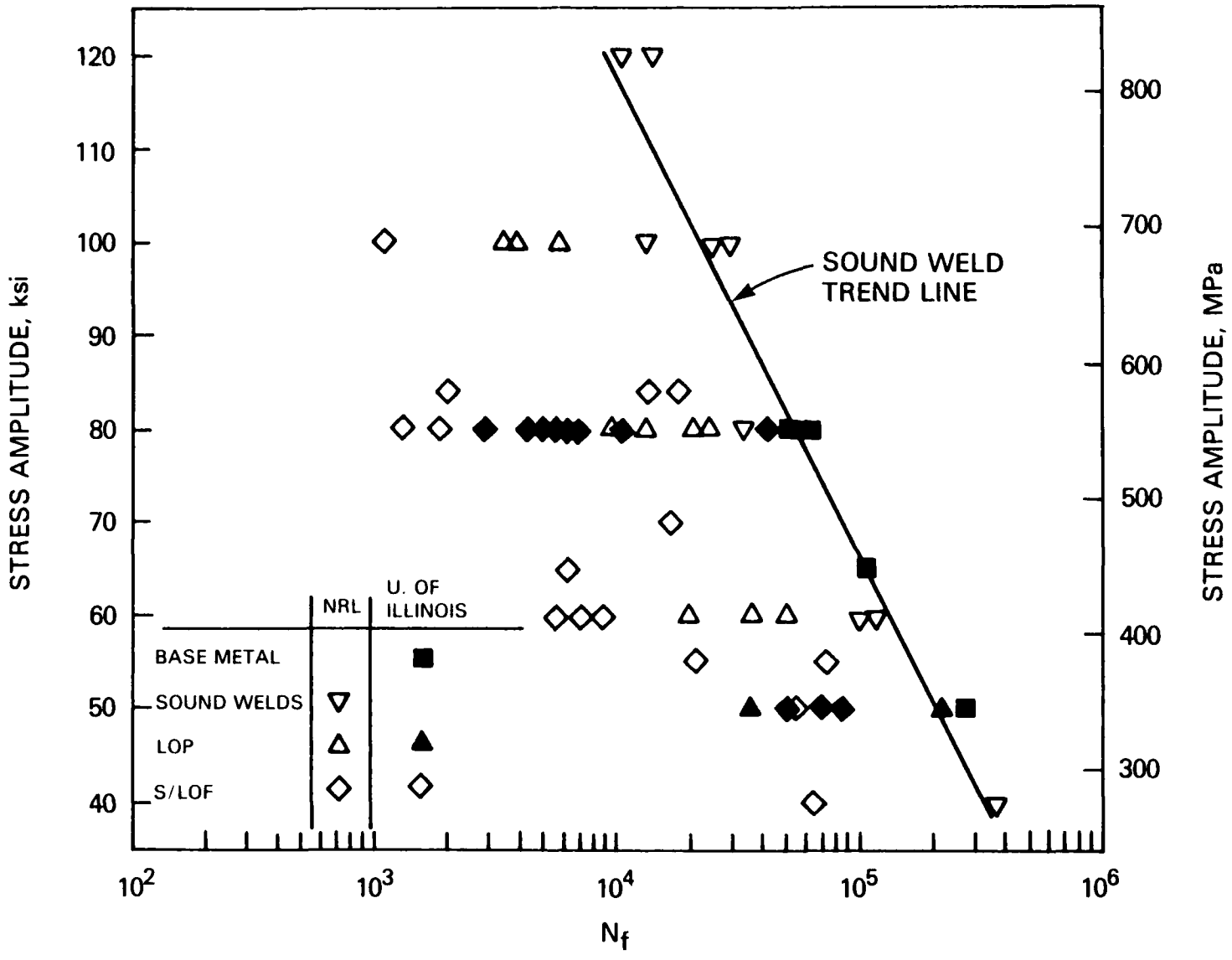

Fig. 2 - Total fatigue life of weldments.

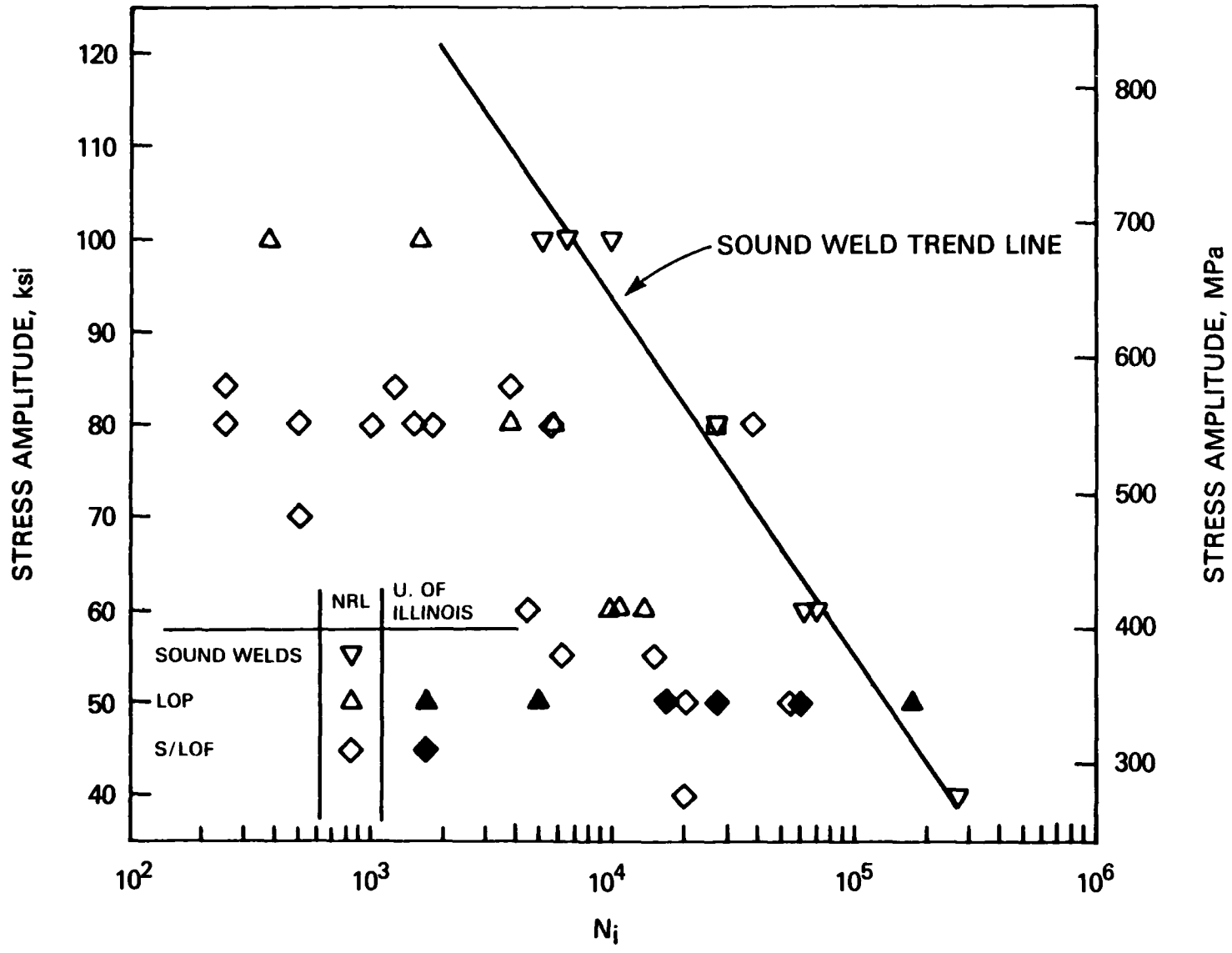

Fig. 3 - Fatigue initiation life of weldments.

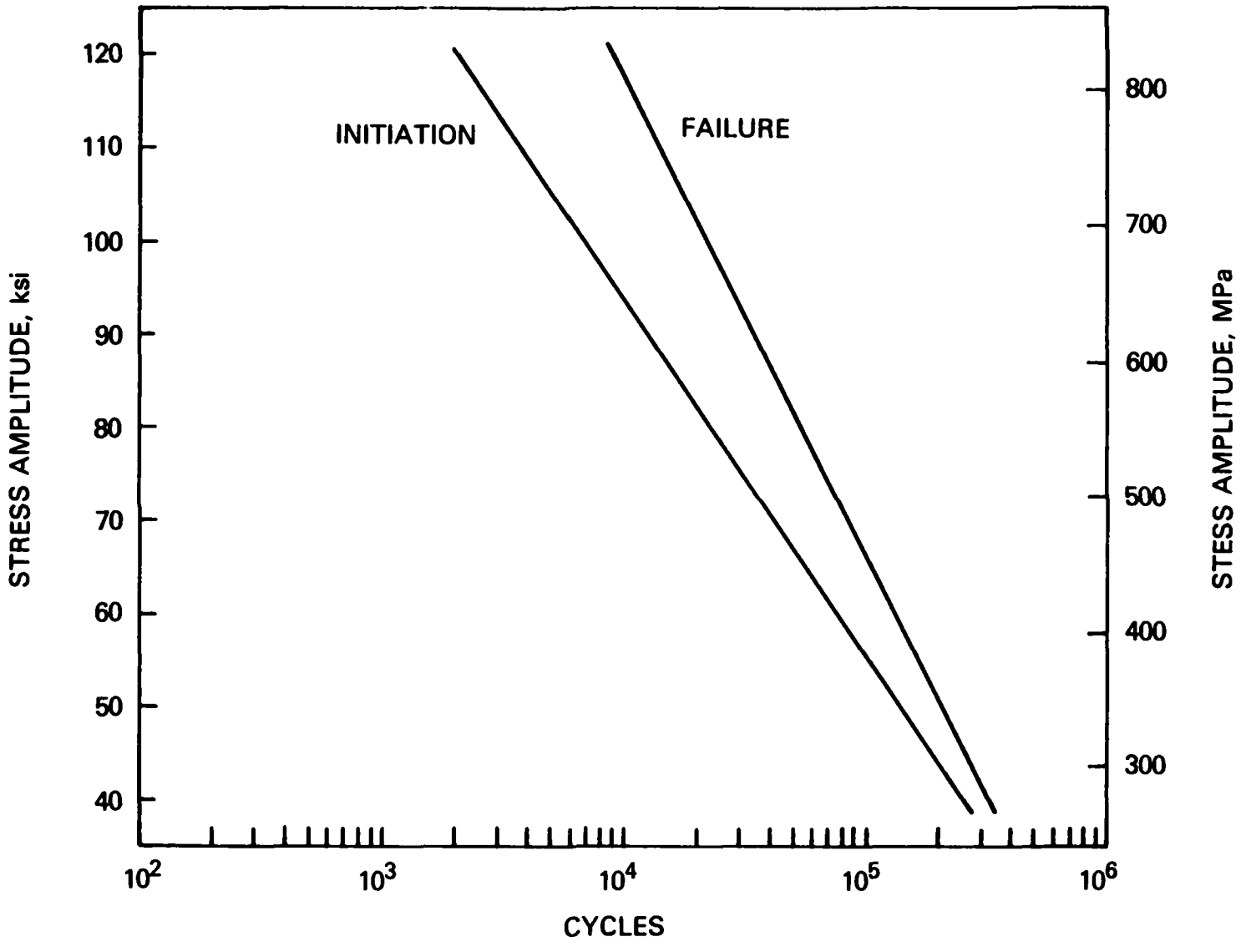

Fig. 4 - Trend lines for fatigue initiation and total fatigue life.

Fig. 5 - Typical lack-of-penetration discontinuity.

Fig. 6 - Typical slag/lack-of-fusion discontinuity.

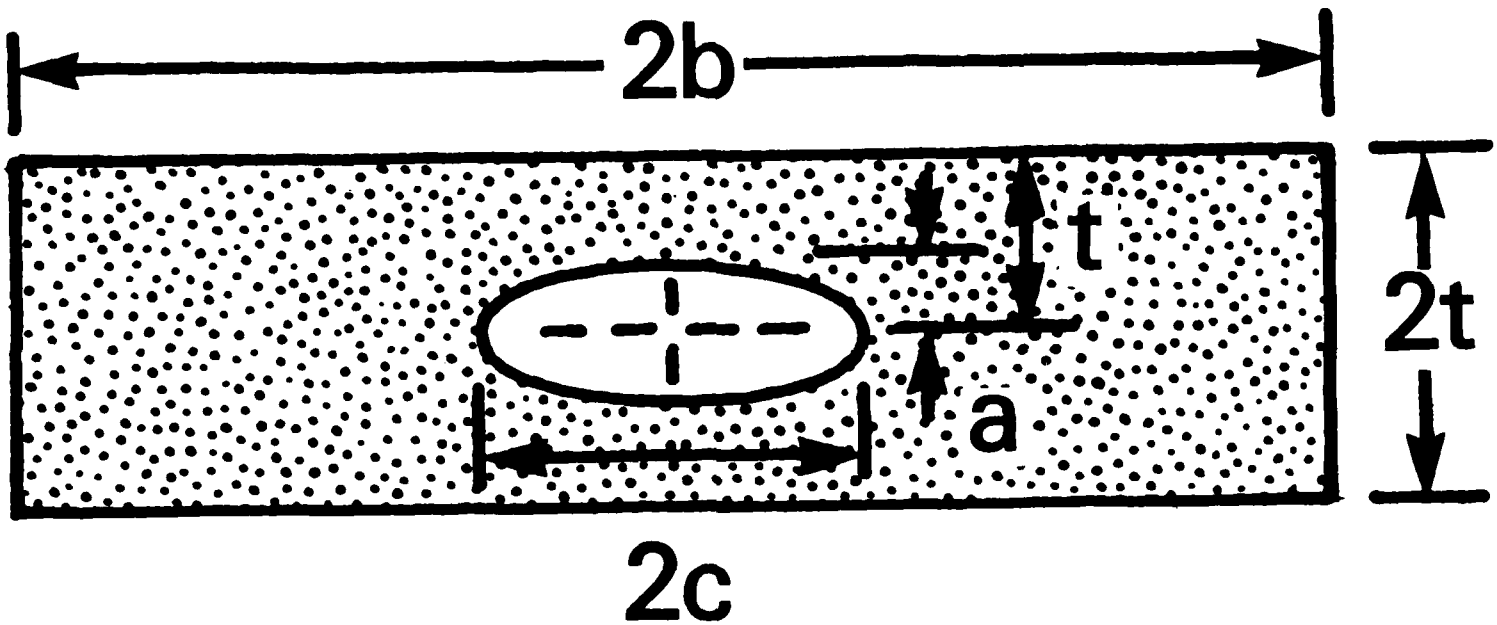

Fig. 7 - Coordinate system used to define dimensions of embedded elliptical discontinuities.

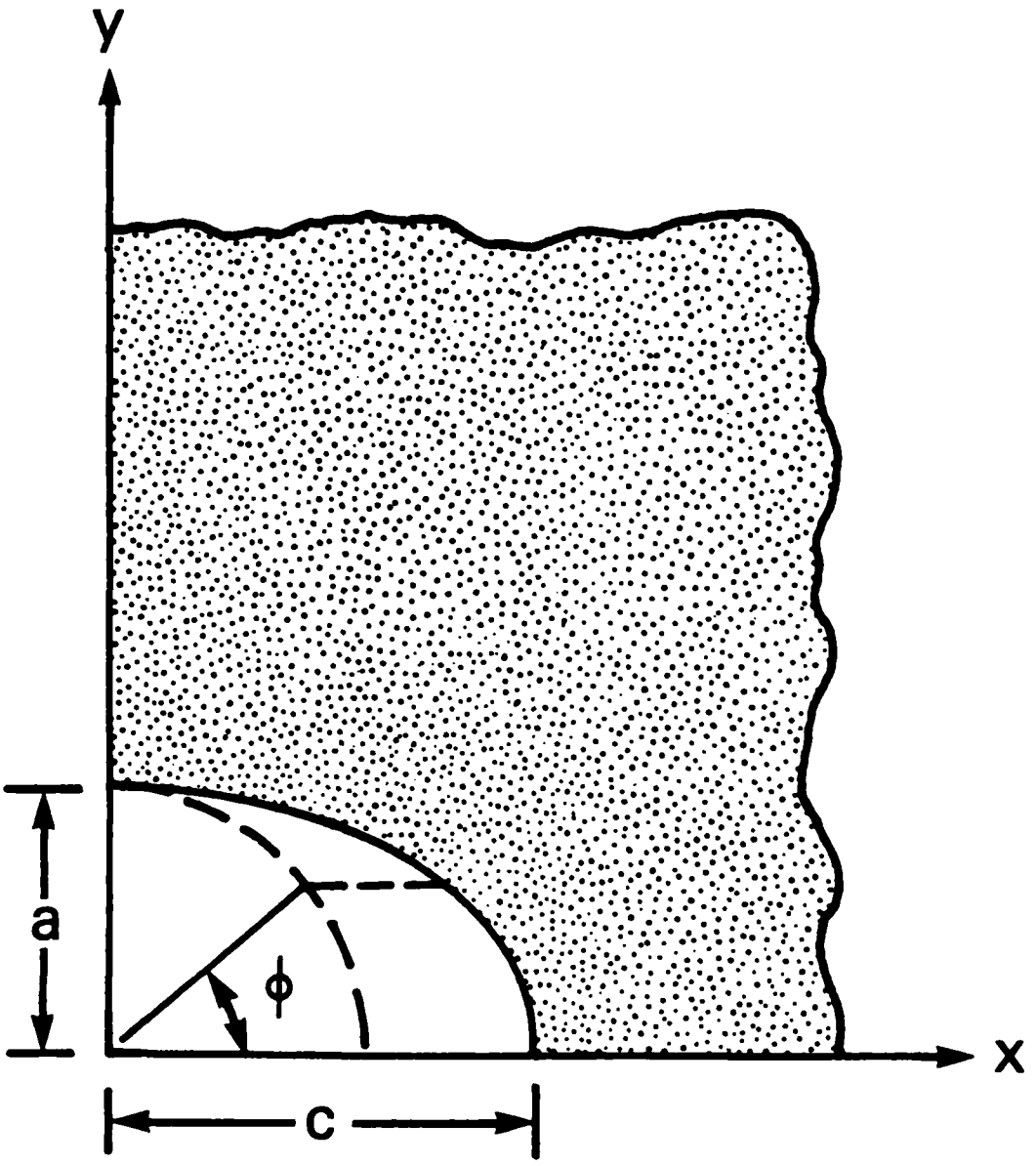

Fig. 8 - Coordinate system used to define the parametric angle for embedded elliptical discontinuities when a/c < 1.

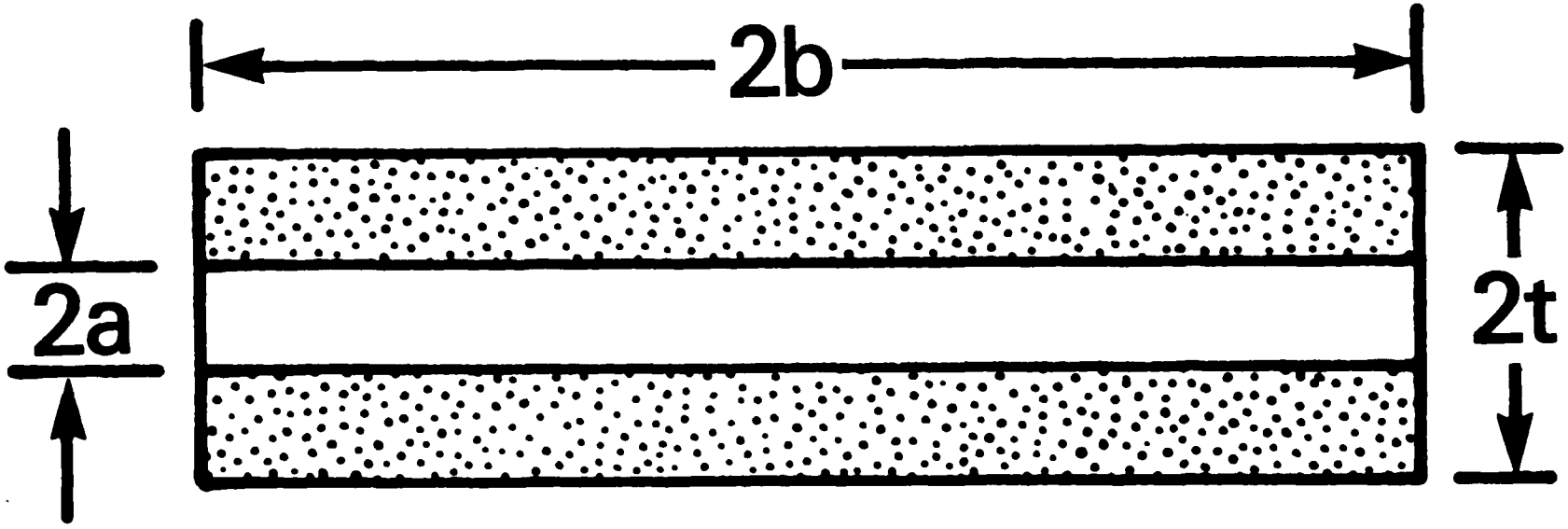

Fig. 9 - Coordinate system used to define dimensions of a through discontinuity in a finite body.

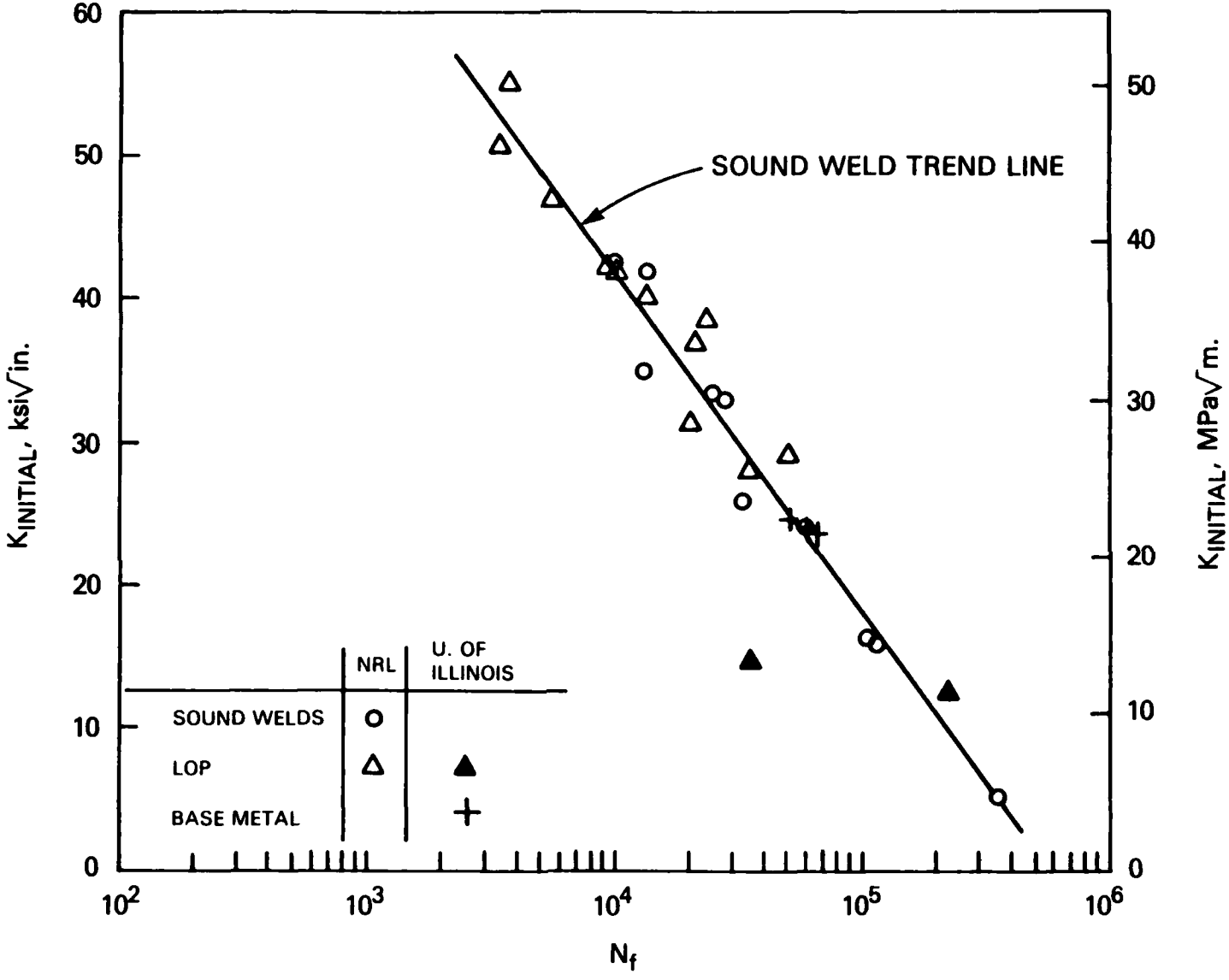

Fig. 10 - Total fatigue life versus initial stress intensity for specimens containing lack-of-penetration discontinuities.

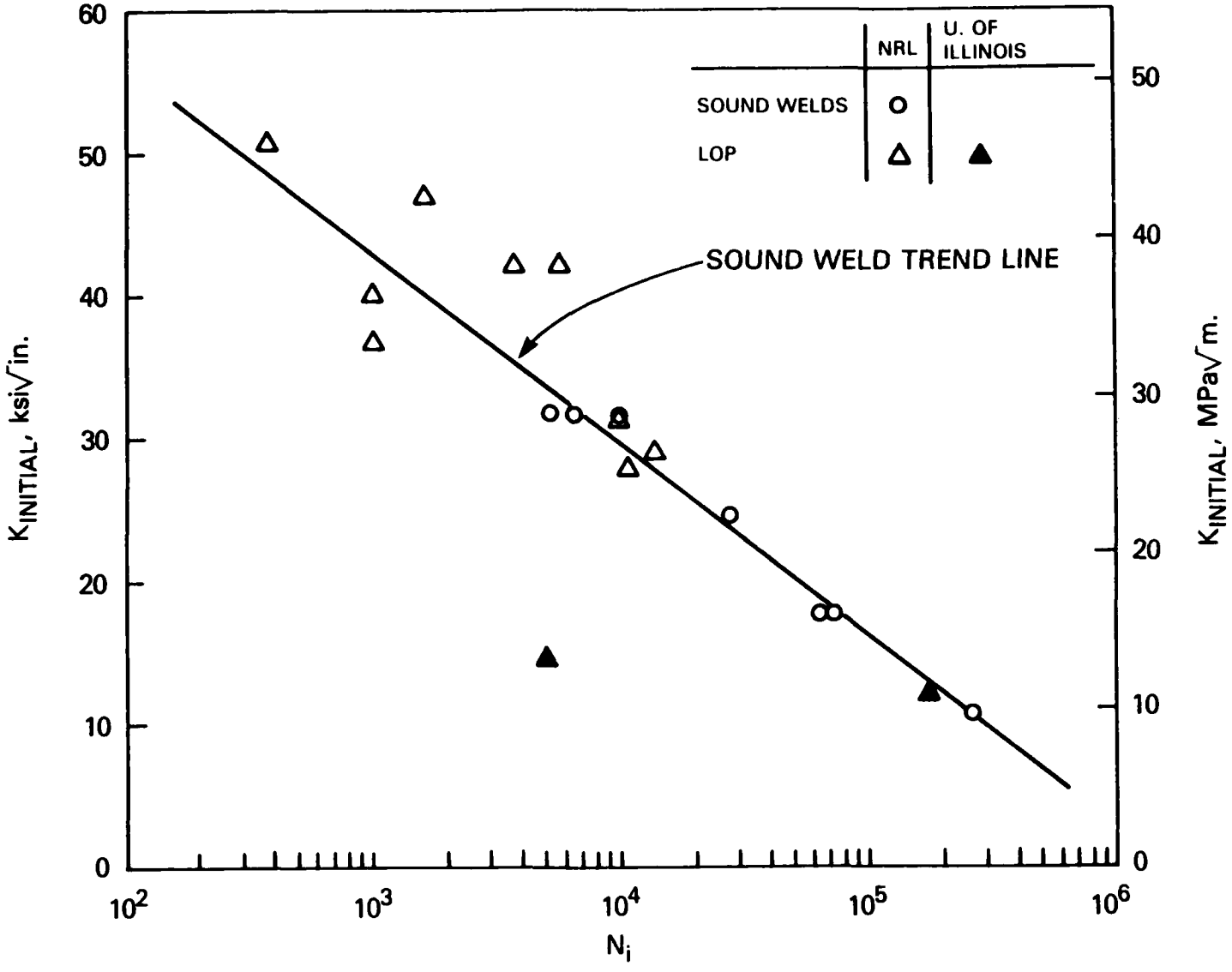

Fig. 11 - Strain gage estimates of fatigue initiation life versus initial stress intensity for specimens containing lack-of-penetration discontinuities.

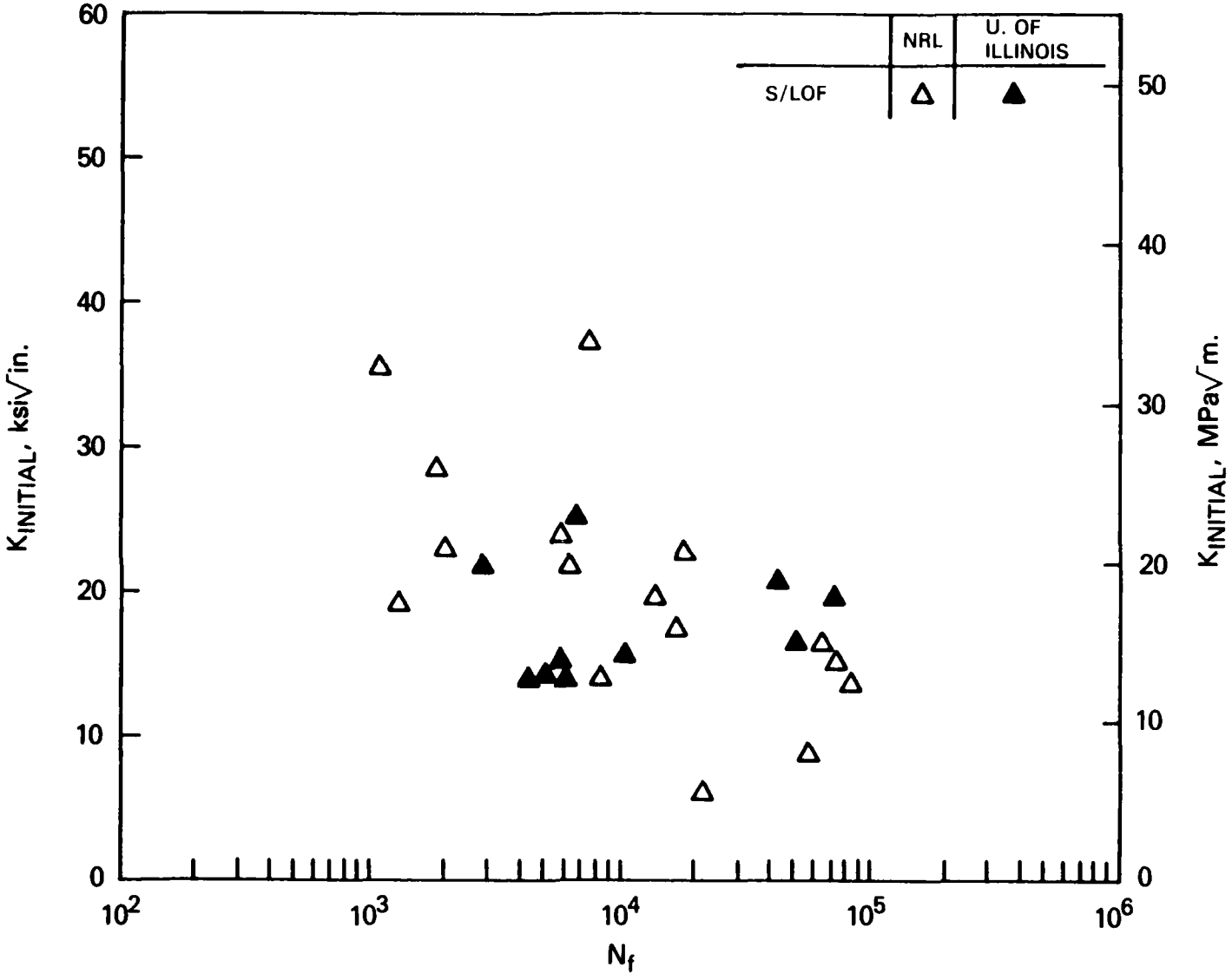

Fig. 12 - Total fatigue life versus initial stress intensity for specimens containing slag/lack-of-fusion discontinuities.

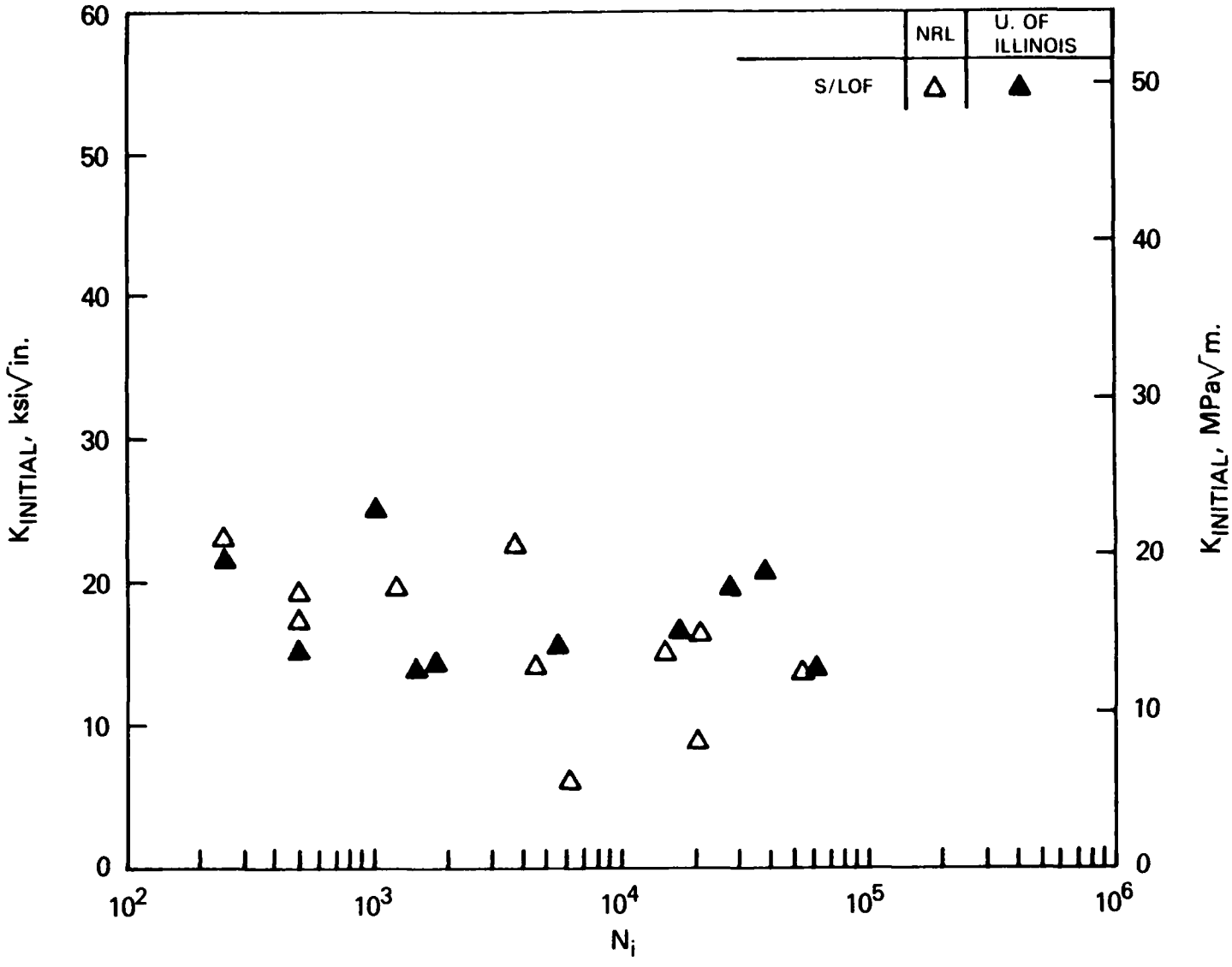

Fig. 13 - Strain gage estimates of fatigue initiation life versus initial stress intensity for specimens containing slag/lack-of-fusion discontinuities.

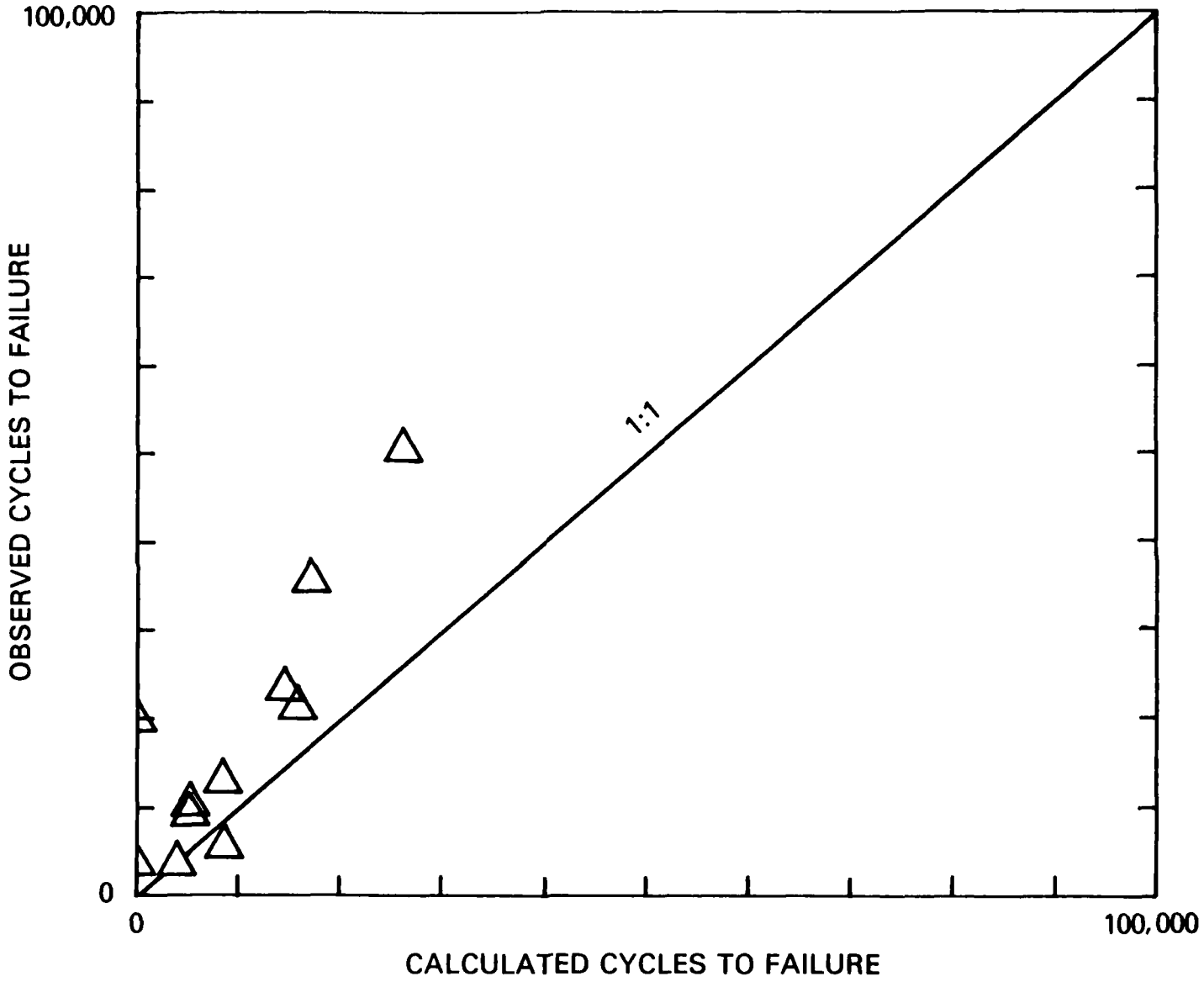

Fig. 14 - Observed versus calculated cycles to failure for specimens containing lack-of-penetration discontinuities.

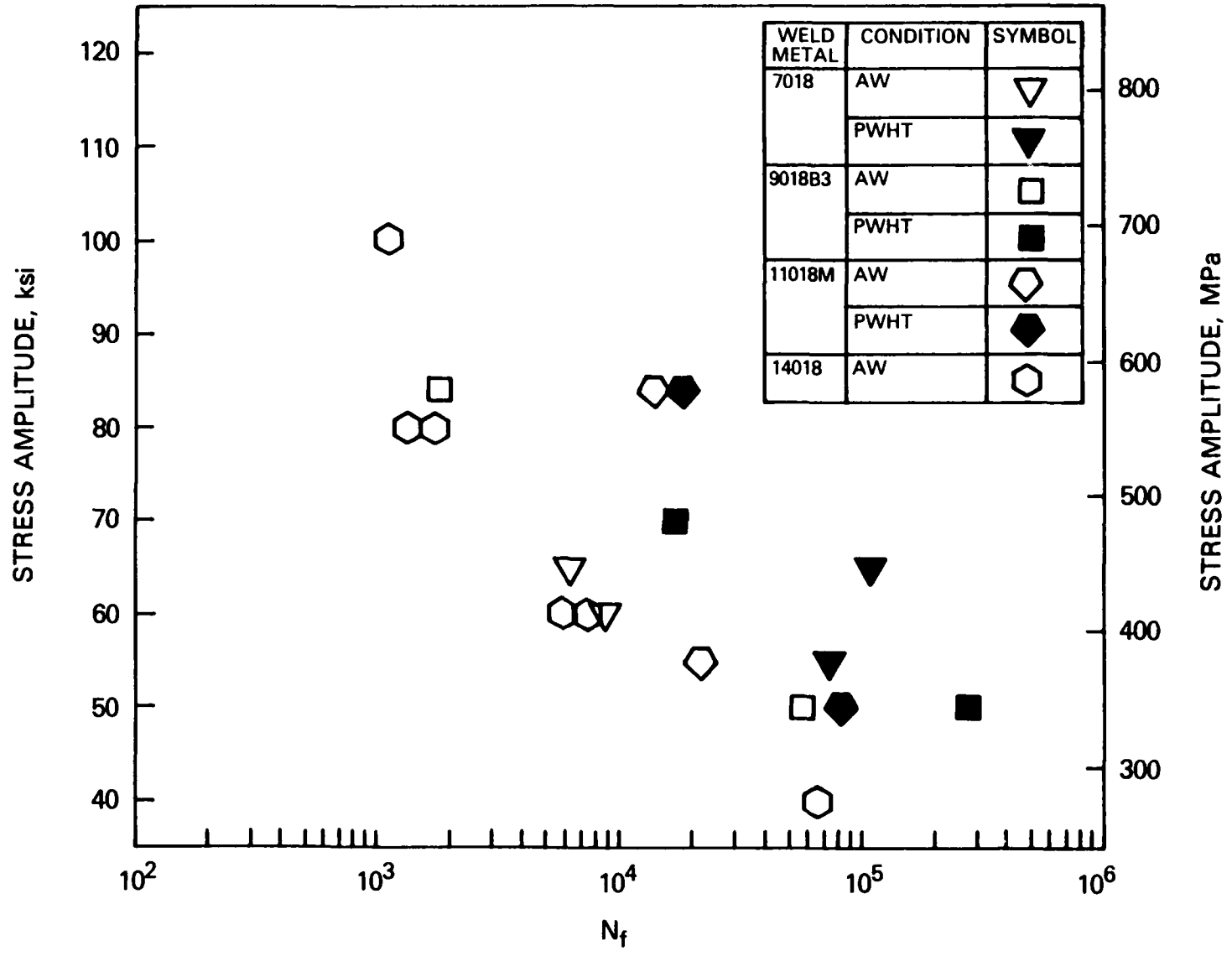

Fig. 15 - Cycles to failure versus stress for specimens containing slag/lack-of-fusion discontinuities.

END

FILMED

6-85

DTIC